Growth and Characterization of Highly Branched Nanostructures of Magnetic Nanoparticles

Yiwen Chu,[†] Jianhua Hu,[†] Wuli Yang,[†] Changchun Wang,*[,†,§] and Jin Z. Zhang*[,‡,||]

Key Laboratory of Molecular Engineering of Polymers (Minister of Education) and Department of Macromolecular Science, Fudan University, Shanghai 200433, China, and Department of Chemistry, University of California, 1156 High Street, Santa Cruz, California 95064

Received: November 10, 2005; In Final Form: January 1, 2006

Magnetite nanoparticles of Fe_3O_4 have been found to grow into large highly branched nanostructures including nanochains and highly branched nanotrees in the solid state through a postannealing process. By varying the preparation conditions such as annealing time and temperature, the nanostructures could be easily manipulated. Changing the starting concentration of the magnetic nanoparticle solution also caused significant changes of the nanoarchitectures. When the magnetic nanoparticle concentration is low, the nanoparticles formed straight rods mainly with an average diameter of 80 nm and a length of several microns. With increasing concentration of the nanoparticles, treelike structures began to form. With further increase of the concentration, well-ordered nanostructures with the appearance of snowflakes were generated. The driving force for the formation of the highly ordered nanostructures includes interaction between the nanoparticles and interaction through surface-capping molecules. This experiment demonstrates that novel nanostructures can be generated by self-assembly of magnetic nanoparticles under the solid state.

I. Introduction

Because of the widespread applications of magnetic nanoparticles, especially in data storage and biomedical areas, such as cell separation,[1] site-specific drug delivery,[2] tissue engineering,[3] and nucleic acid concentration,[4] much attention has been paid to the preparation of different kinds of magnetic nanoparticles in the past decades. To date, a number of preparation methods for magnetic nanoparticles have been developed, such as chemical coprecipitation,[5] inversed microemulsion,[6] ultrasound irradiation,[7] laser pyrolysis,[8] and thermal decomposition.[9] Although monodispersed magnetic nanoparticles have been synthesized using some of these methods, precise control of their size, shape, and surface is generally challenging. Recently, there is a genuine need for fabrication of different dimensional structures of magnetic nanoparticles through self-assembly using nanoscale building blocks.[10]

In the 1980s, several research groups predicted that the monodispersed magnetite nanoparticles could self-assemble to 1D nanostructures in a zero field.[11] But this prediction was not realized in experiments for a long time. The main reason is that well-dispersed magnetic nanoparticles were difficult to prepare. Recently, a thermal decomposition technique offered the opportunity to prepare high-quality magnetic nanocrystals. For example, Sun et al.[9a] have succeeded in synthesizing monodispersed magnetite nanoparticles using $Fe(acac)_3$ as the feed. Because the thermal decomposition technique could provide good controlled size and shape of magnetite nanoparticles, a 1D nanochain of magnetic nanoparticles was observed in solution,[12] and this was also the first time that the 1D structure of magnetic nanoparticles was observed in a zero field by synthesized magnetite nanoparticles.

Furthermore, self-assembly of magnetic nanoparticles is of considerable interest for both fundamental research and applications since they provide direct bridges between nanometer-scale objects and the macroscale devices.[13] The integrity of the building blocks based on self-assembly might provide an intriguing strategy for designing frameworks with desirable shapes and sizes. Using magnetic nanoparticles as building blocks, many larger or higher-order magnetic nanostructures have been prepared.[14] However, to our knowledge, there have been no reports on preparing self-standing nanostructures under solid-state conditions.

In this paper, we fabricated, for the first time, self-standing magnetic nanostructures using a postannealing method. Under this condition, the magnetic nanoparticles could be assembled under solid state. By changing the preparation conditions, different interesting magnetic nanostructures have been obtained. Possible mechanisms responsible for the nanostructure growth are proposed.

II. Experimental Section

Chemicals. $Fe(acac)_3$ (acac = acetylacetonate) was purchased from Shanghai Suocheng Chemical Co. Ltd, vinyl pyrrolidone (VPD) was purchased were from Fluka, and diphenyl ether was purchased from Shanghai Chemical Reagent Co. Ltd.

Preparation of Magnetite Nanoparticles. A typical synthesis procedure of iron oxide nanoparticles is described as follows: 40 mL of diphenyl ether was charged into a flask with a mechanical stirrer and condenser, and then the diphenyl ether was purged with nitrogen to remove oxygen and then heated to 240 °C. A solution of $Fe(acac)_3$ (1.78 g, 5 mmol), vinyl pyrrolidone (5 mL), and diphenyl ether (45 mL) was charged

* Corresponding authors.
[†] Fudan University.
[‡] University of California.
[§] Tel: 86-21-65642385. Fax: 86-21-65640293. E-mail: ccwang@fudan.edu.cn.
[||] Tel: 1-831-459-3776. Fax: 1-831-459-2935. E-mail: zhang@chemistry.ucsc.edu.

10.1021/jp056506r CCC: $33.50
Published on Web 01/27/2006 PAGE EST: 4.4

SCHEME 1: Synthetic Route of Water-Dispersible Magnetite Nanoparticles

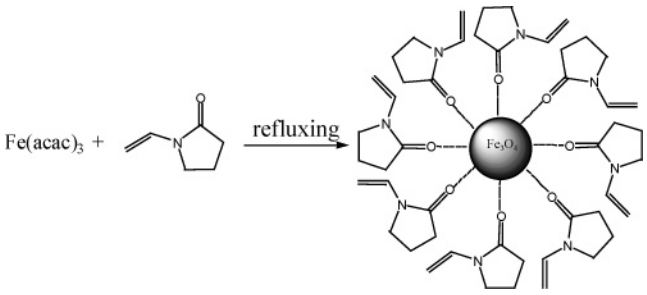

into the flask quickly, and heating of this reaction system was continued for 30 min; then the reaction system was cooled to room temperature by air. With the addition of methanol into the solution, a dark-brown precipitate was obtained; the precipitate was washed several times with acetone and then redispersed in deionized water for further use.

Fabrication of the Nanostructure through a Postannealing Method. To begin, different concentrations of magnetite nanocrystal solution were prepared. A small drop of magnetite nanocrystal solution was placed on a TEM grid, leaving it to dry. The as-deposited thin film was then annealed at 200 °C for a fixed period of time, the sample surface was sputter-coated with gold, and then the self-assembled nanostructures were examined by TEM or SEM.

Instruments and Measurements. High-resolution transmission electron microscopy (HR-TEM) images were obtained on a JEOL JEM2011 electron microscope operating at 200 kV. Scanning electron microscopy (SEM) measurement was carried out on a Philips XL30 microscope, and the samples were loaded onto a copper grid coated with carbon; the sample surface was sputter-coated with a homogeneous gold layer before measurement. Powder X-ray diffraction (XRD) patterns were obtained on a Rigaku D/MAXIIA diffractometer using Cu KR radiation. TGA measurements were carried out on a Perkin-Elmer Pyris-1 series thermal analysis system under a flowing nitrogen atmosphere at a scan rate of 10 °C/min from 100 to 900 °C.

III. Results and Discussion

Scheme 1 illustrates the overall synthesis procedure for magnetite (Fe_3O_4) nanoparticles. For preparation of self-standing magnetic nanostructures, different concentrations of magnetite nanoparticle solution were prepared at first. Then a small drop of the magnetite nanoparticle solution was placed on a carbon-coated copper grid and left to dry. After that, the as-prepared copper grid was annealed in an oven at 200 °C for a fixed amount of time. Finally, the sample was taken out of the oven and examined by HR-TEM or SEM.

Figure 1 shows HR-TEM and SEM images of the as-prepared sample that was annealed at 200 °C for 1 h. Treelike nanostructures, standing on the surface of copper grid, were obtained. From the HR-TEM images of Figure 1, parts a and b, it can be seen that each treelike nanostructure consists of many magnetite nanoparticles. The overall shape of the magnetite nanostructures can be more easily seen in Figure 1c. The highly branched structure is in one plane, stretched upward in air, and standing on the substrate. The selected area electron diffraction (ED) pattern (Figure 1d) shows a highly crystalline nature of magnetite nanoparticle network. In addition, some discrete light spots could be found in the ED pattern, which suggests preferential orientations of magnetite nanoparticles in the chain network. The X-ray diffraction (XRD) pattern of a typical

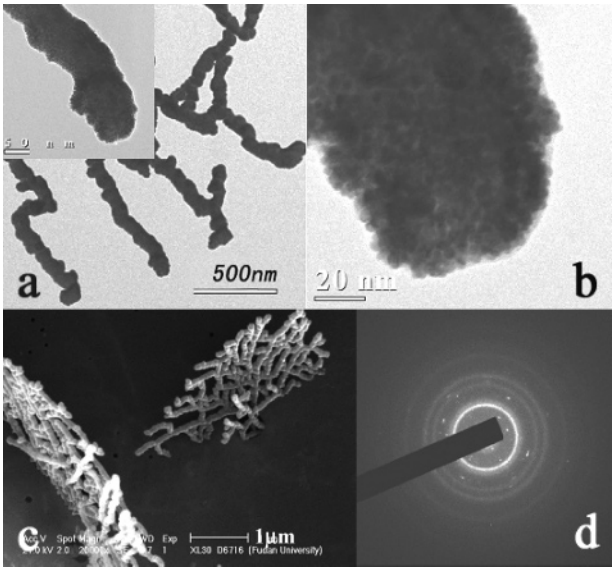

Figure 1. (a) HR-TEM and (c) SEM images of the treelike nanostructures; (b) highly magnified nanostructures of sample (a); (d) selected area electron diffraction from Fe_3O_4 treelike nanostructures.

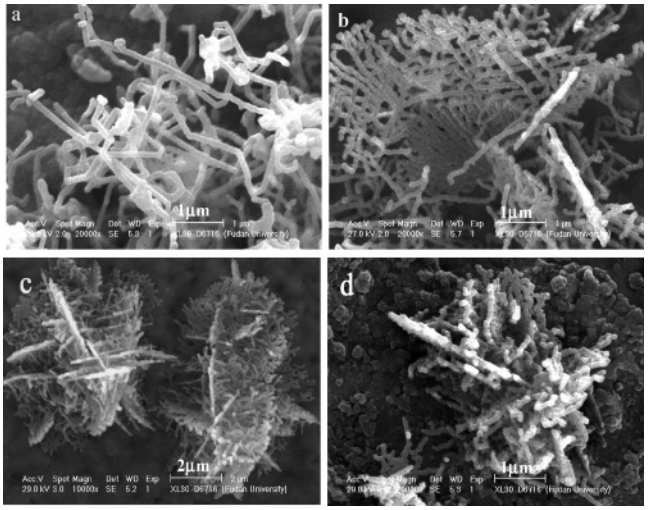

Figure 2. SEM images of the highly branched nanostructures obtained at the same annealing time (1h, 200 °C) but different concentrations: (a) 0.02 g/L, (b) 0.10 g/L, (c) 0.25 g/L, (d) 0.50 g/L.

TABLE 1: Comparison of *d*-Spacing Values of the Synthesized Magnetite Nanocrystals (before and after annealing) with Standard JCPDS Fe_3O_4 Data

d (standard)	2.967	2.532	2.099	1.714	1.615	1.484	1.280
d (expt. before annealing)	2.976	2.532	2.102	1.712	1.615	1.484	1.280
d (expt. after annealing)	2.949	2.514	2.085	1.705	1.605	1.474	1.274

magnetite nanostructure has also been recorded. In the XRD pattern, the positions and relative intensities of all diffraction peaks match the JCPDS card (19-0629) of magnetite (see Table 1) very well. The average particle size calculated using Scherrer's equation is about 12.5 nm. TGA analysis showed that the weight loss of the magnetite nanocrystals is 8.78%, and the decomposing temperature for the ligand (pyrrolidone) is 385 °C, which is much higher than the boiling temperature of vinyl pyrrolidone (215 °C). This result indicates that the vinyl pyrrolidone coordinated with magnetic nanoparticles.

Changes of starting concentration of the magnetic nanoparticle solution have been found to cause variations in the architectures of the magnetite nanostructures. Using the dilute magnetic nanoparticle solution as 0.02 g/L, the Fe_3O_4 nanoparticles mainly

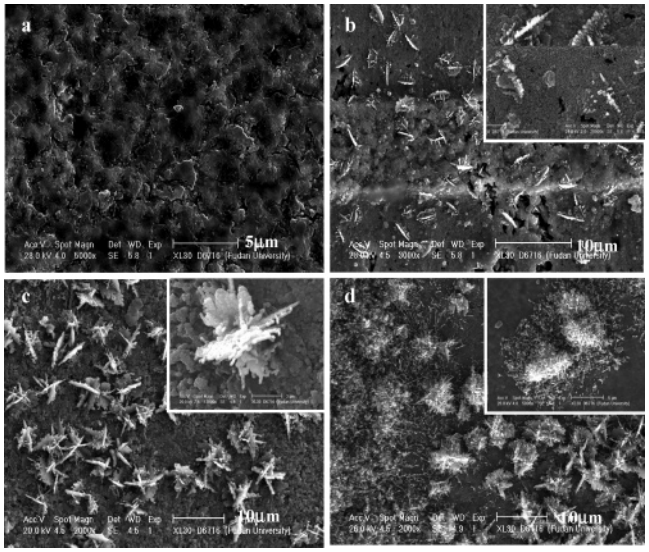

Figure 3. SEM images of the highly branched nanostructures obtained at the same concentration and temperature (0.25 g/L, 200 °C) but different annealing time: (a) 0 h, (b) 1 h, (c) 3 h, (d) 7.5 h.

formed straight rods in disorder as shown in Figure 2a. The average diameter of the rods was about 80 nm, and the length is several microns. With increasing concentration of magnetic nanoparticles, the treelike structures were formed and the density of the branch increased as well (Figure 2, parts b−d). At the concentration of 0.25 g/L, the nanostructures of the magnetic nanoparticles developed ordered structures such as flaky dendrite (Figure 2c).

The annealing time is another very important factor that affects the architecture of the nanostructure formed. When a drop of the magnetic solution was placed on a carbon-coated copper grid, no special structure could be observed before annealing (Figure 3a). Upon annealing in the oven, the special nanostructures grew gradually with annealing time. After annealing for1 h (Figure 3b), the treelike structures were found from SEM. Further annealing of the sample for up to 3 h results in further growth of the nanostructures (Figure 3c). When the annealing time was as long as 7.5 h, most of the nanostructures grew to a very large size and the whole structures collapsed due to overweight and broke into many smaller nanostructures including short magnetic nanorods (see Figure 3d).

The different stages of growth of the nanostructures have also been observed, as shown in Figure 4. The experimental details were the following. A magnetic nanoparticle solution with a concentration of 0.13 g/L was used to prepare a film on a copper grid. The magnetic particle film was annealed at 200 °C for 1 h. Figure 4i is the lower-magnified image; in this image, we could find many magnetic clusters at different growing stages, the details showing in Figure 4, parts a−h. Before the growth, many magnetite nanoparticles aggregate into a cluster with ill-defined structure (see Figure 4a). After annealing, some special structures were formed gradually on the nanoparticle aggregates just as seen in Figure 4, parts b−d, and these structures grew further with annealing and formed flake structures, the flakes linked to each other to form more complicated 3D structures (Figure 4, parts e−h).

The mechanism responsible for the growth of the highly branched magnetite nanostructures is believed to be related to the ligand (VPD) on the particle surface as well as to interaction between particles. When the magnetic nanoparticle solution was simply placed on the copper grid and allowed to dry without annealing by heat, the nanoparticles would aggregate on the surface of the copper grid randomly and could not move. With heating during annealing, the mobility of the nanoparticles increased with increasing temperature and, in the meantime, the surface molecules of VPD could function as a lubricant layer to accelerate the movement of the nanoparticles. Due to dipole−dipole interaction,[12] the nanoparticles could reposition themselves to form new and larger structures to reduce their surface energy.[15] At the same time, the good match between the

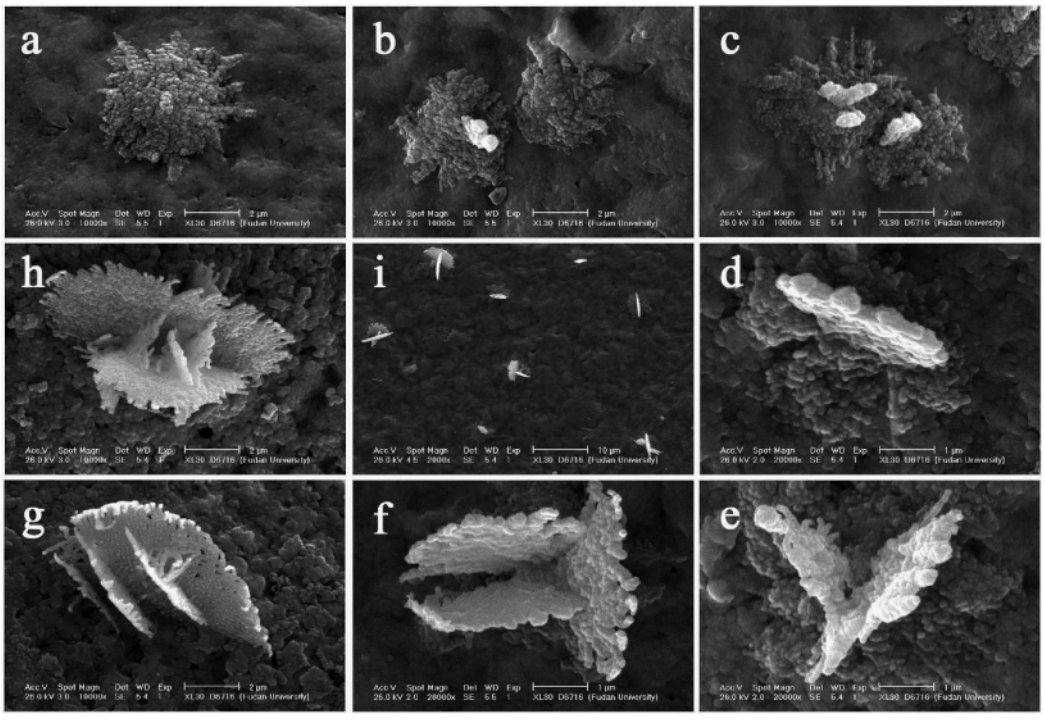

Figure 4. SEM images of Fe_3O_4 nanostructures under different growing stages. (The concentration of magnetite nanoparticle solution is 0.13 g/L, the copper grid with dried nanoparticle film was annealed at 200 °C for 1 h.) (a) Stage I: Magnetite nanoparticles aggregated together and formed clusters. (b−d) Stage II: Special structures were growing. (e−h) Stage III: Flake structures were formed.

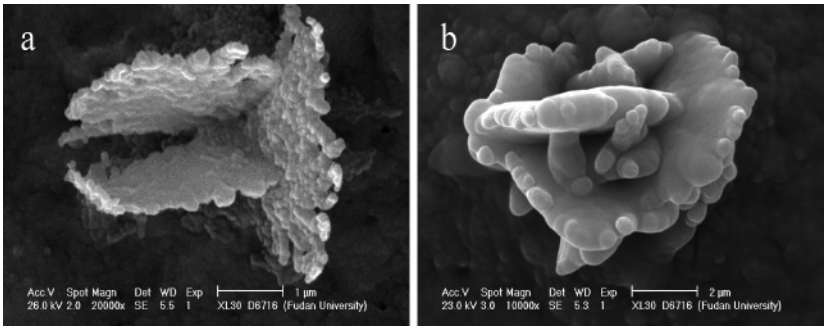

Figure 5. SEM images of (a) highly branched nanostructures obtained at 200 °C for 1 h (the magnetic solution is 0.13 g/L), and (b) sample (a) coated with a gold layer and annealed for another 1 h.

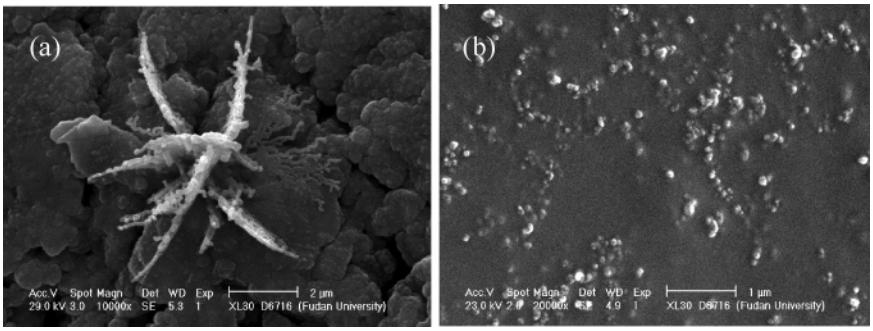

Figure 6. SEM images of Fe_3O_4 nanostructures under annealing at 200 °C for 1 h; (a) the ligand is pyrrolidone, and (b) the ligand is oleic acid.

boundaries of magnetite nanoparticles in the formed large nanostructures seems to suggest that the growth mechanism also involves preferred orientation or reorientation of the nanoparticles during the growth of the large branched nanostructure.[10c] Particularly, at 200 °C the driving force is strong enough to cause rearrangement of the nanoparticles in the structures, as can be seen in Figure 5. Figure 5a shows the nanostructures of a sample (see Figure 4f) annealed at 200 °C for 1 h, and the detailed structure of each flake could be distinguished clearly. By further annealing this sample at 200 °C for 1 h (Figure 5b), the flakes disappeared and the surface of the nanostructure became more smooth. This is likely because the surface of the nanostructures had been coated with a gold layer for SEM observation for the first 1 h of annealing; the movement of the nanoparticles was confined during further annealing. This indicates that the flake still grew under further annealing even under the gold-layer coating, which shows that the driving force for growing is very strong.

In our experiment, we also tested the influence of temperature and ligands on the special nanostructures. Generally, an annealing temperature >150 °C is favorable for forming the nanostructures, and when the temperature is <150 °C, no highly branched nanostructure could be formed. By replacing vinyl pyrrolidone with pyrrolidone, similar assemble morphology could be obtained (see Figure 6a). If the vinyl pyrrolidone was replaced with oleic acid, no highly branched nanostucture could be obtained under our experimental conditions (see Figure 6b).

Magnetic properties of the magnetic nanoparticles were investigated by a VSM (vibrating sample magnetometer) before and after annealing, and the hysteresis loops of the dried magnetic samples have been recorded. Figure 7 is the magnetization curve of the sample which indicates that the magnetic nanoparticles are superparamagnetic before annealing; that is, when the applied magnetic field is removed, the sample keeps no remanence and the saturation magnetization is about 71.2 emu/g. After annealing, the magnetic nanoparticles were not superparamagnetic, and the maximum magnetization (59.0 emu/g) is lower than that before annealing. This indicates that some changes of the magnetic nanoparticles have taken place during the annealing process. The positions and relative intensities of all diffraction peaks did not change after annealing (see Table 1). However, we found that a dispersion peak formed after annealing, indicating that some amorphous ferrite oxide formed.

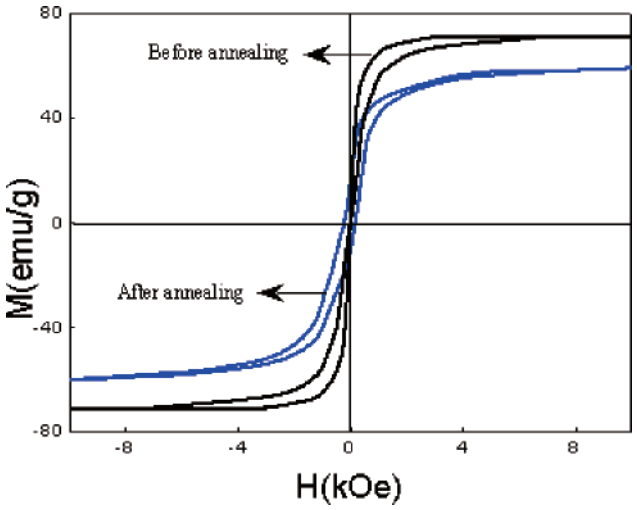

Figure 7. Room-temperature magnetization curves of magnetite nanocrystals before and after annealing.

IV. Conclusion

A series of interesting highly branched and self-standing magnetic nanostructures were fabricated using a postannealing method. The preparation conditions, such as annealing temperature, annealing time, and the concentration of the magnetic nanoparticle solution, have a significant influence on the structure of the final structures. When the magnetic nanoparticle concentration is low, the nanoparticles mainly formed straight rods with an average diameter of 80 nm and a length of several microns. With increasing concentration of the nanoparticles,

treelike structures started to form. With further increase of the concentration, ordered nanostructures with the appearance of flaky dendrites were generated. This approach has the virtues of simplicity, reproducibility, and high yield. It provides a new method for producing novel nanostructures under solid-state conditions.

Acknowledgment. This work was supported by the National Science Foundation of China (Grant Nos. 20374012, 50173005) and the National Science Fund for Distinguished Young Scholars of China (50525310). J.Z.Z. is grateful for the support of the Advanced Scholars Program of Fudan University.

Supporting Information Available: TGA and differential curves of the magnetite (Fe_3O_4) nanoparticles; and powder X-ray diffraction patterns of synthesized Fe_3O_4 magnetite nanoparticle before and after annealing. This material is available free of charge via the Internet at http:// pubs.acs.org.

References and Notes

(1) (a) Ugelstad, J.; Berge, A.; Ellingsen, T.; Schmid, R.; Nilsen, T.-N.; Mork, P. C.; Stenstad, P.; Hornes, E.; Olsvik, O. *Prog. Polym. Sci.* **1992**, *17*, 87. (b) Molday, R. S.; Yen, S. P. S.; Rembaum, A. *Nature* **1977**, *268*, 437. (c) Rembaum, A.; Dreyer, W. J. *Science* **1980**, *208*, 364.

(2) (a) Viroonchatapan, E.; Ueno, M.; Sato, H.; Adachi, I.; Nagae, H.; Tazawa, K.; Horikoshi, I. *Pharm. Res.* **1995**, *12*, 1176. (b) Gupta, P. K.; Hung, C. T. *Life Sci.* **1989**, *44*, 175.

(3) Kim, D. K.; Zhang, Y.; Voit, W.; Rao, K. V.; Kehr, J.; Bjelke, B.; Muhammed, M. *Scr. Mater.* **2001**, *44*, 1713.

(4) (a) Uhlen, M. *Nature* **1989**, *340*, 733. (b) Elaissari, M.; Rodrigue, M.; Meunier, F.; Herve, C. *J. Magn. Magn. Mater.* **2001**, *225*, 127.

(5) Harris, L. A.; Goff, J. D.; Carmichael, A. Y.; Riffle, J. S.; Harburn, J. J.; Pierre, T. G. S.; Saunders, M. *Chem. Mater.* **2003**, *15*, 1367.

(6) Mann, S.; Sparks, H. C.; Board, R. G. *Adv. Microbiol. Physiol.* **1990**, *31*, 125.

(7) Kumar, R. V.; Koltypin, Y.; Xu, X. N.; Yeshurun, Y.; Gedanken, A.; Felner, I. *J. Appl. Phys.* **2001**, *89*, 6324.

(8) Verdaguer, S. V.; Miguel, O. B.; Morales, M. P. *Scr. Mater.* **2002**, *47*, 589.

(9) (a) Sun, S. H.; Zeng, H. *J. Am. Chem. Soc.* **2002**, *124*, 8204. (b) Park, J.; An, K.; Hwang, Y.; Park, J.-G.; Noh, H.-J.; Kim, J. Y.; Park, J.-H.; Hwang, N.-M.; Hyeon, T. *Nat. Mater.* **2004**, *3*, 891. (c) Park, J.; Lee, E.; Hwang, N. M.; Kang, M.; Kim, S. C.; Hwang, Y.; Park, J. G.; Noh, H. J.; Kim, J. Y.; Park, J. H.; Hyeon, T. *Angew. Chem., Int. Ed.* **2005**, *44*, 2872.

(10) . (a) Nikhi, J. R.; Peng, X. G. *J. Am. Chem. Soc.* **2003**, *125*, 14280. (b) Gao, X.; Yu, K. M. K.; Tam, K. Y.; Tsang, S. C. *Chem. Commun.* **2003**, *24*, 2998. (c) Lee, H.; Purdon, A. M.; Chu, V.; Westervelt, R. M. *Nano Lett.* **2004**, *4*, 995.

(11) (a) Chantrell, R. W.; Bradbury, A.; Popplewell, J.; Charles, S. W. *J. Phys. D: Appl. Phys.* **1980**, *13*, L119. (b) Teixeira, P. I. C.; Tavares, J. M.; da Gama, M. M. T. *J. Phys.: Condens. Matter.* **2000**, *12*, R411.

(12) (a) Butter, K.; Bomans, P. H. H.; Frederick, P. M.; Vroege, G. J.; Philipse, A. P. *Nat. Mater.* **2003**, *2*, 88. (b) Klokkenburg, M.; Vonk, C.; Claesson, E. M.; Meeldijk, J. D.; Erné, B. H.; Philipse, A. P. *J. Am. Chem. Soc.* **2004**, *126*, 16706.

(13) (a) Lisiecki, I.; Albouy, P.; Pileni, M. *Adv. Mater.* **2003**, *15*, 712. (b) Courty, A.; Fermon, C.; Pileni, M. *Adv. Mater.* **2001**, *13*, 254.

(14) (a) Hou, Y.; Kondoh, H.; Shimojo, M.; Sako, E. O.; Ozaki, N.; Kogure, T.; Ohta, T. *J. Phys. Chem.* **2005**, *109*, 4845. (b) Goubault, C.; Leal-Calderon, F.; Viovy, J.-L.; Bibette, J. *Langmuir* **2005**, *21*, 3725.

(15) Alivisatos, A. P. *Science* **2000**, *289*, 736.